Extinction and the optical theorem. Part II. Multiple particles

Matthew J. Berg, Christopher M. Sorensen,* and Amitabha Chakrabarti

Department of Physics, Kansas State University, Manhattan, Kansas 66506-2601, USA
**Corresponding author: sor@phys.ksu.edu*

Received November 9, 2007; revised April 10, 2008; accepted April 16, 2008;
posted April 21, 2008 (Doc. ID 89533); published June 4, 2008

The extinction due to a group of identical particles in a fixed orientation is studied. An analytical description based on the Maxwell volume integral equation is presented, describing the interference energy flow due to a group of noninteracting identical particles. As compared to a single particle, the effect of multiple particles is shown to narrow the angular region around the forward direction over which the dominant contribution to the group's extinction cross section occurs. The extinction due to a group of fully interacting nonspherical particles is studied using the discrete dipole approximation. Interparticle interactions are found not to change the essential character of the interference-based energy flow mechanism that describes extinction. © 2008 Optical Society of America

OCIS codes: 290.2200, 290.5850, 290.1310, 260.3160, 000.2690.

1. INTRODUCTION

Part I of this work examines the extinction caused by a single particle [1]. There it is shown how the interference between the incident and the scattered waves establishes a radially alternating energy flow that yields the particle's extinction cross section C^{ext} when integrated over all directions. This article extends the analysis of Part I to systems of multiple particles. The following will demonstrate how the presence of multiple particles causes the dominant contribution to C^{ext} to occur in an angular region that narrows with increasing particle group size. The key result of this work will be to demonstrate that all of the essential conclusions made in Part I, regarding the mechanism and meaning of extinction, apply to the multiparticle groups.

Section 2 presents a theoretical description of the extinction due to a group of identical, noninteracting particles. Section 3 shows simulations of the interference energy flow due to several types of noninteracting particle groups. Interacting particles are examined in Section 4, and their corresponding extinction is compared to that of noninteracting particles. The work is concluded in Section 5.

2. EXTINCTION BY A NONINTERACTING MULTIPARTICLE GROUP

Here a group of identical particles will be examined in the noninteracting particle approximation. In reality, there is always some degree of interaction between the particles, and the effect of this interaction will be addressed in Section 4. By considering noninteracting particles first, one is most easily able to compare to the results presented in Part I. The conditions required to minimize the interactions between the particles in a group are presented in [2–5]. These conditions are reviewed here to make the work more self-contained and to illustrate the limits of validity of the approximations used.

Consider a group of N identical particles residing in vacuum. The distribution of the particles is time independent but otherwise arbitrary. Let R_{sc} be the radius of the smallest circumscribing sphere that encloses any single one of the N particles, and let m be the particles' refractive index. The origin of the laboratory coordinate system is located near the geometric center of a particle, and this particle will be referred to as the primary particle $i=1$; see Fig. 1(a). The location of the ith particle is given by the vector $\mathbf{R}_i$, which connects the origin of the primary particle $\mathcal{O}_1$ to that of the ith particle, $\mathcal{O}_i$. Let R_{gr} be the radius of the smallest circumscribing sphere that encloses the entire N-particle group. The observation point $\mathbf{r}$ is assumed to be located far enough from the group that it satisfies the far-field conditions of [6] with respect to *both* the group and each constituent particle.

Let R_{min} be the minimum interparticle separation; see Fig. 1(b). The particles will be considered essentially noninteracting if

$$k(R_{min}-R_{sc})\gg 1, \tag{1}$$

$$R_{min}\gg R_{sc}, \tag{2}$$

$$kR_{min}\gg \frac{k^2R_{sc}^2}{2}. \tag{3}$$

The conditions that establish that the observation point is in the far-field zone of the entire group are given by [6] as

$$k(r-R_{gr})\gg 1, \tag{4}$$

$$r\gg R_{gr}, \tag{5}$$

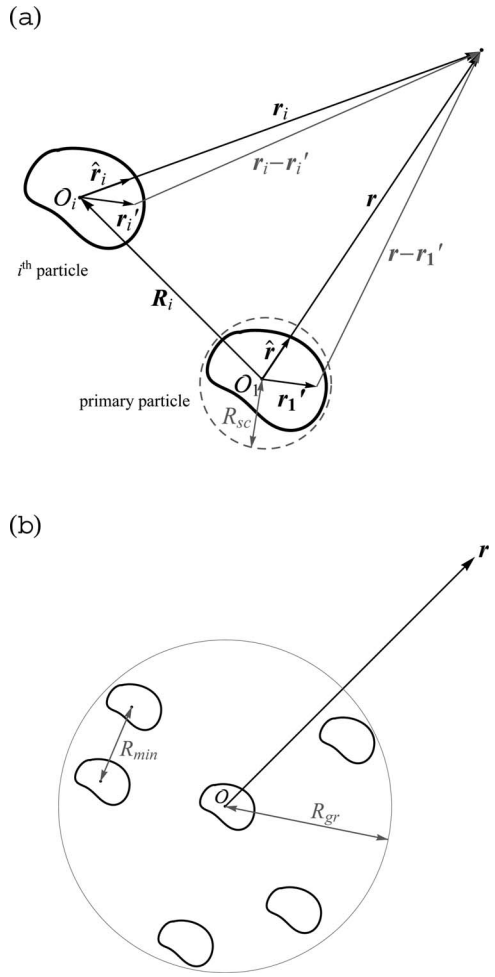

Fig. 1. (a) Sketch of the primary particle and the ith particle of a multiparticle group. (b) Sketch illustrating the definition of the particle group's circumscribing sphere radius R_{gr} and the minimum interparticle separation R_{min}.

$$kr \gg \frac{k^2 R_{gr}^2}{2}. \tag{6}$$

The inequalities of Eqs. (1)–(6) correspond to the so-called far-field single-scattering approximation (SSA), where the entire group effectively acts as a single pointlike particle [3,5].

A consequence of the identical particle SSA is that the far-field scattered wave due to the group can be formulated in terms of the wave scattered by the primary particle only. To describe how this is done, denote the primary particle as $i=1$ and consider the volume integral equation (VIE) giving the scattered electric field for *any* external location,

$$\mathbf{E}_1^{sca}(\mathbf{r}) = k^2(m^2-1)\int_{V_1} \overleftrightarrow{G}(\mathbf{r},\mathbf{r}_1') \cdot \mathbf{E}_1^{int}(\mathbf{r}_1')\mathrm{d}\mathbf{r}_1'. \tag{7}$$

Here V_1 and $\mathbf{E}_1^{int}$ denote the volume and internal electric field of the primary particle, respectively, and

$$\overleftrightarrow{G}(\mathbf{r},\mathbf{r}') = \left(\overleftrightarrow{I} + \frac{1}{k^2}\nabla \otimes \nabla\right)\frac{\exp(ik|\mathbf{r}-\mathbf{r}'|)}{4\pi|\mathbf{r}-\mathbf{r}'|} \tag{8}$$

is the free-space dyadic Green's function [3,7]. Note that Eq. (7) is valid at any point $\mathbf{r}$, not just in the far-field zone. The task now is to determine how the electric field inside the ith particle ($i \neq 1$) is related to $\mathbf{E}_1^{int}$. This can be done using the dyadic transition operator, which relates the incident field inside a particle to its scattered wave as

$$\mathbf{E}_1^{sca}(\mathbf{r}) = \int_{V_1} \overleftrightarrow{G}(\mathbf{r},\mathbf{r}_1') \cdot \int_{V_1} \overleftrightarrow{T}(\mathbf{r}_1',\mathbf{r}_1'') \cdot \mathbf{E}^{inc}(\mathbf{r}_1'')\mathrm{d}\mathbf{r}_1''\mathrm{d}\mathbf{r}_1', \quad \mathbf{r} \in \mathbb{R}^3, \tag{9}$$

where

$$\overleftrightarrow{T}(\mathbf{r}_1,\mathbf{r}_1') = k^2(m^2-1)\delta(\mathbf{r}_1-\mathbf{r}_1')\overleftrightarrow{I} + k^2(m^2-1) \times \int_{V_1} \overleftrightarrow{G}(\mathbf{r}_1,\mathbf{r}_1'') \cdot \overleftrightarrow{T}(\mathbf{r}_1'',\mathbf{r}_1')\mathrm{d}\mathbf{r}_1'', \quad \mathbf{r}_1,\mathbf{r}_1' \in V_1, \tag{10}$$

see p. 117 of [3]. Comparing Eqs. (7) and (9) shows that the primary particle's internal field obeys

$$k^2(m^2-1)\mathbf{E}_1^{int}(\mathbf{r}_1) = \int_{V_1} \overleftrightarrow{T}(\mathbf{r}_1,\mathbf{r}_1') \cdot \mathbf{E}^{inc}(\mathbf{r}_1')\mathrm{d}\mathbf{r}_1', \quad \mathbf{r}_1 \in V_1. \tag{11}$$

From Eq. (10), one can see that $\overleftrightarrow{T}$ depends on the particle's material properties through m, the vacuum wavelength through k, and the particle's shape and size through the integral over V_1. Notice, however, that $\overleftrightarrow{T}$ must be independent of the choice of origin, since the functions δ and $\overleftrightarrow{G}$ in Eq. (10) do not depend on any specific origin. This gives the translation behavior of the operator as

$$\overleftrightarrow{T}(\mathbf{r}_1,\mathbf{r}_1') = \overleftrightarrow{T}(\mathbf{r}_i,\mathbf{r}_i'), \tag{12}$$

where $\mathbf{r}_i = \mathbf{r} - \mathbf{R}_i$ and $\mathbf{r}_i' = \mathbf{r}_1' + \mathbf{R}_i$; recall Fig. 1(a). Using Eq. (1) of Part I and Eqs. (11) and (12) and Fig. 1(b) from here, the internal electric field at a location $\mathbf{r}_i'$ inside the ith particle is related to the internal field at the corresponding point $\mathbf{r}_1'$ inside the primary particle as

$$\mathbf{E}^{int}(\mathbf{r}_i') = \exp(ik\mathbf{R}_i \cdot \hat{\mathbf{n}}^{inc})\mathbf{E}^{int}(\mathbf{r}_1'), \quad \mathbf{r}_i' \in V_i, \quad \mathbf{r}_1' \in V_1. \tag{13}$$

Now consider the simplification of the dyadic Green's function, Eq. (8), for the ith particle in the SSA. Equation (5) justifies

$$\frac{1}{|\mathbf{r}_i - \mathbf{r}_i'|} \approx \frac{1}{r}, \tag{14}$$

and

$$\hat{\mathbf{r}}_i \approx \hat{\mathbf{r}}, \tag{15}$$

whereas Eqs. (4)–(6) together permit

$$\exp(ik|\mathbf{r}_i - \mathbf{r}_i'|) \approx \exp[ik(r - \mathbf{r}_i' \cdot \hat{\mathbf{r}})]. \tag{16}$$

With the approximations of Eqs. (14)–(16), one can simplify Eq. (8) to

$$\overleftrightarrow{G}(\mathbf{r},\mathbf{r}_i') \approx \frac{1}{4\pi}\frac{e^{ikr}}{r}(\overleftrightarrow{I} - \hat{\mathbf{r}} \otimes \hat{\mathbf{r}})\exp(-ik\mathbf{r}_i' \cdot \hat{\mathbf{r}}), \tag{17}$$

which, from Eq. (7), gives the scattered electric field due to the ith particle as

$$\mathbf{E}_i^{sca}(\mathbf{r}) = \frac{k^2}{4\pi}\frac{e^{ikr}}{r}(m^2 - 1)(\overleftrightarrow{I} - \hat{\mathbf{r}} \otimes \hat{\mathbf{r}}) \cdot \int_{V_i} \mathbf{E}_i^{int}(\mathbf{r}_i') \times \exp(-ik\mathbf{r}_i' \cdot \hat{\mathbf{r}})\mathrm{d}\mathbf{r}_i'. \tag{18}$$

With the use of Eq. (13) and $\mathbf{r}_i' = \mathbf{r}_1' + \mathbf{R}_i$, the integral over the ith particle's volume V_i in Eq. (18) can now be replaced with the integral over the primary particle's volume V_1, giving

$$\mathbf{E}_i^{sca}(\mathbf{r}) = \frac{k^2}{4\pi}\frac{e^{ikr}}{r}(m^2 - 1)\exp[ik\mathbf{R}_i \cdot (\hat{\mathbf{n}}^{inc} - \hat{\mathbf{r}})] \times (\overleftrightarrow{I} - \hat{\mathbf{r}} \otimes \hat{\mathbf{r}}) \cdot \int_{V_1} \mathbf{E}_1^{int}(\mathbf{r}_1')\exp(-ik\mathbf{r}_1' \cdot \hat{\mathbf{r}})\mathrm{d}\mathbf{r}_1'. \tag{19}$$

Equation (19) is equivalent to the far-field scattered electric field given by Eqs. (5) and (7) of Part I, augmented by the phase factor $\exp[ik\mathbf{R}_i \cdot (\hat{\mathbf{n}}^{inc} - \hat{\mathbf{r}})]$. Let the *scattering wave vector* $\mathbf{q}$ be defined as

$$\mathbf{q}(\hat{\mathbf{r}}) = k(\hat{\mathbf{n}}^{inc} - \hat{\mathbf{r}}); \tag{20}$$

then Eq. (19) becomes

$$\mathbf{E}_i^{sca}(\mathbf{r}) = \exp[i\mathbf{q}(\hat{\mathbf{r}}) \cdot \mathbf{R}_i]\mathbf{E}_1^{sca}(\mathbf{r}), \tag{21}$$

which gives the scattered electric field of the ith particle in terms of that of the primary particle. The net wave scattered by the entire noninteracting particle group is then given by

$$\mathbf{E}_{gr}^{sca}(\mathbf{r}) = \frac{\exp(ikr)}{r}\mathbf{E}_o^{sca}(\hat{\mathbf{r}})\sum_{i=1}^{N}\exp[i\mathbf{q}(\hat{\mathbf{r}}) \cdot \mathbf{R}_i], \tag{22}$$

$$\mathbf{B}_{gr}^{sca}(\mathbf{r}) = \frac{k}{\omega}\frac{\exp(ikr)}{r}\hat{\mathbf{r}} \times \mathbf{E}_o^{sca}(\hat{\mathbf{r}})\sum_{i=1}^{N}\exp[i\mathbf{q}(\hat{\mathbf{r}}) \cdot \mathbf{R}_i], \tag{23}$$

where $\mathbf{E}_o^{sca}$ is the single-particle scattering amplitude of Eq. (7) of Part I. The interference term in the Poynting vector that describes the extinction due to the particle group follows from Eqs. (1) and (2) of Part I and Eqs. (22) and (23) above as

$$\langle \mathbf{S}_{gr}^{cross}(\mathbf{r})\rangle_t = \frac{1}{2\mu_o}\mathrm{Re}\{\mathbf{E}^{inc}(\mathbf{r}) \times [\mathbf{B}_{gr}^{sca}(\mathbf{r})]^* + \mathbf{E}_{gr}^{sca}(\mathbf{r}) \times [\mathbf{B}^{inc}(\mathbf{r})]^*\}. \tag{24}$$

Following the same analysis as in Part I, the structure of $\langle \mathbf{S}_{gr}^{cross}\rangle_t$ is examined by surrounding the group by the large imaginary spherical surface $\mathcal{S}_l$ of radius R_l centered on the origin. The size of this surface is large enough that points on it satisfy the far-field conditions of Eqs. (4)–(6). The intersection of $\mathcal{S}_l$ with the plane containing the origin and perpendicular to the polarization of the incident electric field defines the contour $\mathcal{C}_l$. Integration of the radial component of the interference energy flow of Eq. (24) over $\mathcal{S}_l$ and normalization by the intensity of the incident wave I^{inc} gives the group's extinction cross section as

$$C_{gr}^{ext} = -\frac{1}{I^{inc}}\oint_{\mathcal{S}_l}\langle \mathbf{S}_{gr}^{cross}(\mathbf{r})\rangle_t \cdot \hat{\mathbf{r}}\mathrm{d}S. \tag{25}$$

This is a direct generalization of Eqs. (12) and (17) of Part I, which give the single-particle cross section C^{ext}. Application of the optical theorem [Eq. (22) of Part I] to Eq. (22) above shows that

$$C_{gr}^{ext} = NC^{ext}. \tag{26}$$

Equation (26) is the classic result that the total extinction cross section C_{gr}^{ext} for a group of noninteracting particles is the sum of each particle's cross sections independently; see [8] and Subsection 7.2 of [3]. Notice that the calculations above demonstrate that the additivity of the cross sections *does not* rely on any assumption that the spatial distribution of the particles be random, as is assumed in [8]. The form of Eqs. (22) and (23) shows that the particle group's scattered wave is a transverse spherical wave in the far-field zone. Consequently, the same interference mechanism that enables the redistribution of energy in the extinction caused by a single particle applies to a noninteracting multiparticle group. The only difference between single-particle and multiparticle extinction in this case is the appearance of the phase-factor sum in Eqs. (22) and (23).

Using Eqs. (1) and (2) of Part I and Eqs. (22), (23), and (25) above, one finds that the radial component of the interference energy flow through the $\mathcal{C}_l$ contour is

$$\langle \mathbf{S}_{gr}^{cross}(R_l\hat{\mathbf{r}})\rangle_t \cdot \hat{\mathbf{r}} = \frac{c_o}{R_l}K(\hat{\mathbf{r}})\mathrm{Re}\{f_o(\hat{\mathbf{r}})f_{gr}(\hat{\mathbf{r}}) \times \exp[ikR_l(1 - \hat{\mathbf{r}} \cdot \hat{\mathbf{n}}^{inc})]\}, \quad \mathbf{r} \in \mathcal{C}_l, \tag{27}$$

where

$$f_{gr}(\hat{\mathbf{r}}) = \sum_{i=1}^{N}\exp[i\mathbf{q}(\hat{\mathbf{r}}) \cdot \mathbf{R}_i]. \tag{28}$$

When compared to the corresponding single-particle energy flow of Eq. (24) of Part I, Eq. (27) reveals that the spatial distribution of the particles in the group introduces an additional envelope bounding the alternating radial energy flow, but is otherwise identical.

3. EXAMPLES OF THE EXTINCTION DUE TO A MULTIPARTICLE GROUP

To illustrate the similarities and differences between single-particle and multiparticle extinction in the SSA, simulations of the interference energy flow for a multiparticle group consisting of identical spheres are examined. The size parameter of each sphere is $kR=6.18$, where R is the sphere radius and their refractive index is $m=1.25+0.30i$. The particles are distributed within the group volume in both an ordered and disordered manner. The ordered distribution has the particles centered on a cubic lattice of spacing $R_o=4R$ that fills a spherical volume of radius R_{gr} and is shown in Fig. 2(a), where $N=136$. The disordered distribution is shown in Fig. 2(b) and is generated by displacing the particles in the ordered distribution by a random distance between $-R$ and R along each coordinate axis. The disordered distribution is not intended to be rigorously random in character; rather, its purpose is to demonstrate what effect the structure of the distribution has on the group's extinction. Notice that the interparticle separation of $4R$ for these distributions does not satisfy Eqs. (1)–(3), yet the particles are treated as noninteracting in the simulations anyway. The reason that this is done is due to the excessive computational demands resulting from an attempt to strictly satisfy both Eqs. (1)–(3) and Eqs. (4)–(6) simultaneously. Care is taken, however, to satisfy Eqs. (4)–(6).

The extinction due to the two spherical particle groups is calculated using the Mie solution to the Maxwell equations for a single sphere. The net scattered fields for the entire multiparticle group are then obtained from the single-particle fields through Eqs. (22) and (23). The interference energy flow due to the group is then calculated from Eq. (27).

Consider the analogy to Eq. (28) of Part I for the multiparticle group,

$$\partial C_{gr}^{ext}(\theta_s) = \frac{1}{I^{inc}} \int_{\partial \mathcal{S}_f} \langle \mathbf{S}_{gr}^{cross}(\mathbf{r}) \rangle_t \cdot \hat{\mathbf{r}} \mathrm{d}S, \tag{29}$$

where the surface $\partial \mathcal{S}_f$ is the part of the large spherical surface $\mathcal{S}_l$ extending from the forward direction $\theta=0$ to θ_s, as shown in Fig. 5(b) of Part I. Comparison of Eqs. (25) and (29) shows that $\partial C_{gr}^{ext}(\pi) = -NC^{ext}$ when $\theta_s=\pi$ and the partial surface $\partial \mathcal{S}_f$ closes to coincide with $\mathcal{S}_l$.

Plots of Eq. (29) are shown in Fig. 3 for the ordered and disordered spherical particle groups consisting of $N=1$, 19, and 136 particles. The curves are normalized by the single-particle extinction cross section C^{ext}, and the size of the partial surface $\partial \mathcal{S}_f$ used to render the curves is $R_l=600R_{gr}$. These plots demonstrate the same oscillating behavior as the single-particle simulations in Fig. 4 of Part I. Small detailed differences in the structure of the curves for the ordered and disordered distributions can be found, yet the curves achieve the value for C_{gr}^{ext} expected from Eq. (26) regardless of the distribution's structure. Moreover, the curves show that as the number of particles in the group increases, and hence the group size increases, the dominant contribution to the extinction cross section occurs over a decreasing angular region near the forward direction. The origin of this behavior is explained by the group amplitude profile f_{gr} in Eq. (28), which has the form of a Fourier series and hence narrows in $\mathbf{q}$ as the group grows in extent $\mathbf{R}_i$. More explicitly, f_{gr} of Eq. (28) can be transformed into a Fourier integral as

$$\sum_{i=1}^{N} \exp[i\mathbf{q}(\hat{\mathbf{r}}) \cdot \mathbf{R}_i] \to \frac{1}{V_{gr}} \int_{V_{gr}} \exp[i\mathbf{q}(\hat{\mathbf{r}}) \cdot \mathbf{r}'] \mathrm{d}\mathbf{r}'. \tag{30}$$

This transformation will be valid when $\mathbf{q}(\hat{\mathbf{r}}) \cdot \mathbf{d} \ll 1$, where $\mathbf{d}$ is the maximum nearest-neighbor separation between the particles in the group. From Eq. (20) one can see that this condition essentially restricts $\hat{\mathbf{r}}$ to point near the forward direction $\hat{\mathbf{n}}^{inc}$.

The integral in Eq. (30) can be approximately evaluated in terms of the radius of gyration of the particle group following [9]. The result is

$$f_{gr}(\hat{\mathbf{r}}) \approx 1 - \frac{1}{3}[q(\hat{\mathbf{r}})R_g]^2, \quad \text{for } q(\hat{\mathbf{r}})R_g < 1, \tag{31}$$

where R_g is the group's radius of gyration. If it is now assumed that the particle group is spherical and that the

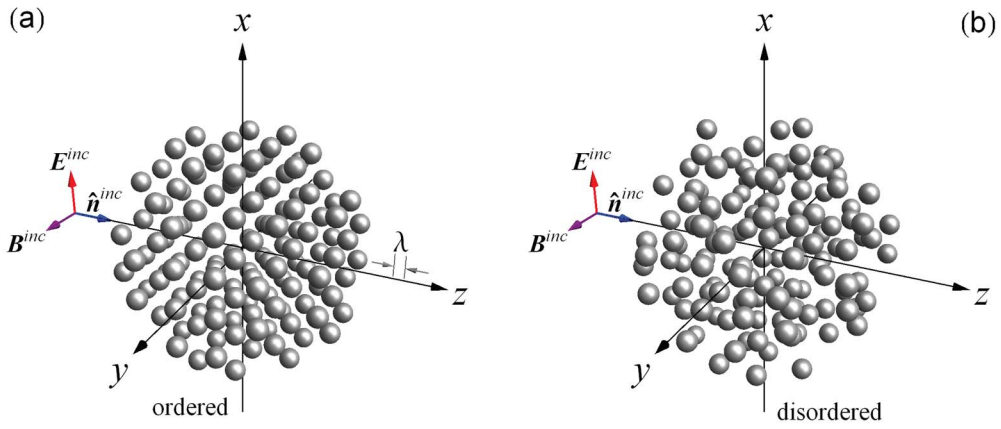

Fig. 2. (Color online) Examples of the ordered (a) and disordered (b) spherical particle distributions used in the simulations of Fig. 3. The total number of particles in both groups is $N=136$, and the vacuum wavelength λ is shown in (a) along the z axis for scale.

distribution of the particles appears approximately uniform on the scale of $1/q$ throughout the group volume, the group's radius of gyration becomes $R_g=\sqrt{3/5}R$; see [10]. Provided that the observation point resides on the $\mathcal{C}_l$ contour near the forward direction, one can use Eqs. (20) and (31) to find the approximate angle $\theta_{2/3}$ at which the magnitude of the interference energy flow of Eq. (24) decreases to two thirds of its value in the forward direction,

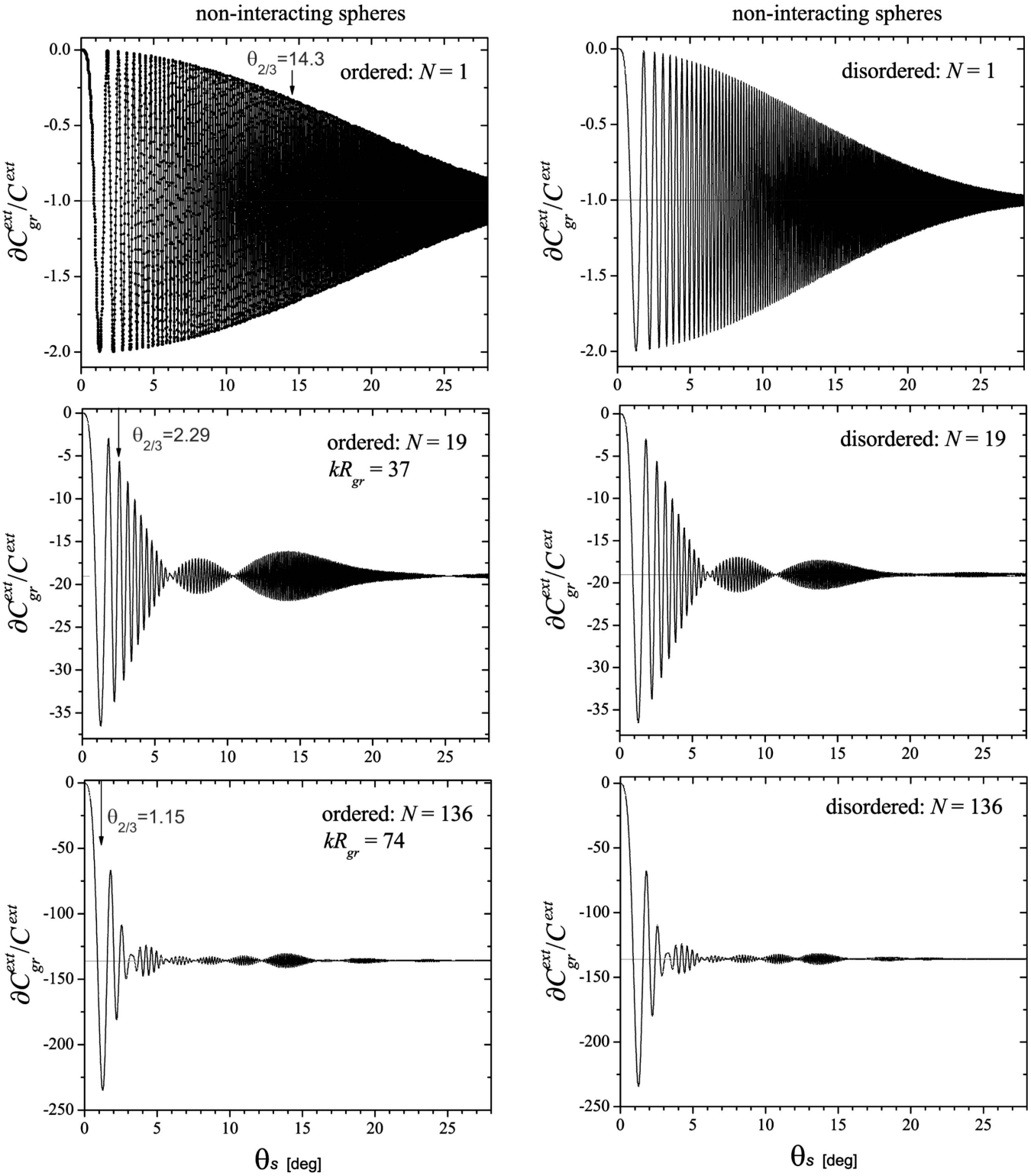

Fig. 3. Plots of the integral ∂C_{gr}^{ext} given in Eq. (29) for the noninteracting ordered and disordered spherical particle groups. In each case the curves are normalized to the extinction cross section of a single particle C^{ext}. The size parameter and refractive index of a single particle is $kR=6.18$ and $m=1.25+0.30i$, respectively.

$$\theta_{2/3} \approx \sqrt{\frac{5}{3}\frac{1}{kR_{gr}}}. \quad (32)$$

The values of $\theta_{2/3}$ are indicated in Fig. 3, where the narrowing of the extinction around the forward direction with increasing group radius is evident.

4. EXAMPLES OF THE EXTINCTION DUE TO AN INTERACTING MULTIPARTICLE GROUP

Up to this point, interactions between the particles of a group have been entirely neglected. Consequently, a strong similarity is found between the behavior of the energy flow due to a single particle and a noninteracting particle group. This section examines a small group of fully interacting particles to see what effects the interparticle interactions have on the extinction mechanism.

The fully interacting particle group considered here is composed of $N=9$ identical, homogeneous cubical particles distributed in a body-centered cubical arrangement; see Fig. 4. The sphere-volume-equivalent size parameter of the individual particles is $kR_{ve}=3.38$, whereas that of the entire group is $kR_{ve}^{gr}=7.02$. The particles' refractive index is $m=1.33+0i$, and they all share the same orientation as shown in Fig. 4.

The discrete dipole approximation (DDA) is used to simulate the group's scattered wave. For a detailed review of the DDA model, see [11]. In short, the DDA numerically solves the VIE for the internal electric field inside each particle, complete with a full account of the interparticle interactions. Once each particle's internal field is known, the group's scattered wave is calculated via Eq. (18), and the interference energy flow $\langle \mathbf{S}_{gr}^{cross}(\mathbf{r})\rangle_t$ follows from Eq. (24).

Figure 5(a) shows the integral ∂C_{gr}^{ext} given by Eq. (29) for the *single* cubical particle located at the origin in Fig. 4 in the absence of its eight neighbors, i.e., without interactions. The curve is normalized by the single-particle extinction cross section C^{ext}, and the radius of the partial surface $\partial\mathcal{S}_f$ is $R_l=10R_{gr}$. This plot is qualitatively identical to Fig. 7 in Part I and the $N=1$ plot in Fig. 3 above. As before, one can see that the interference energy flow must be integrated on $\partial\mathcal{S}_f$ beyond 60° from the forward direction to obtain C^{ext} to better than 10% error.

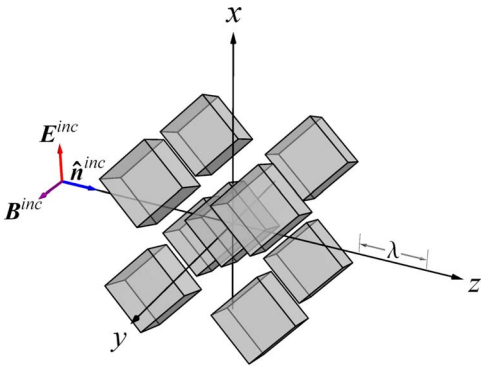

Fig. 4. (Color online) Sketch showing the body-centered cubical arrangement of identical cubical particles corresponding to the integrated energy flow plots shown in Figs. 5 and 6. The vacuum wavelength λ is shown for scale.

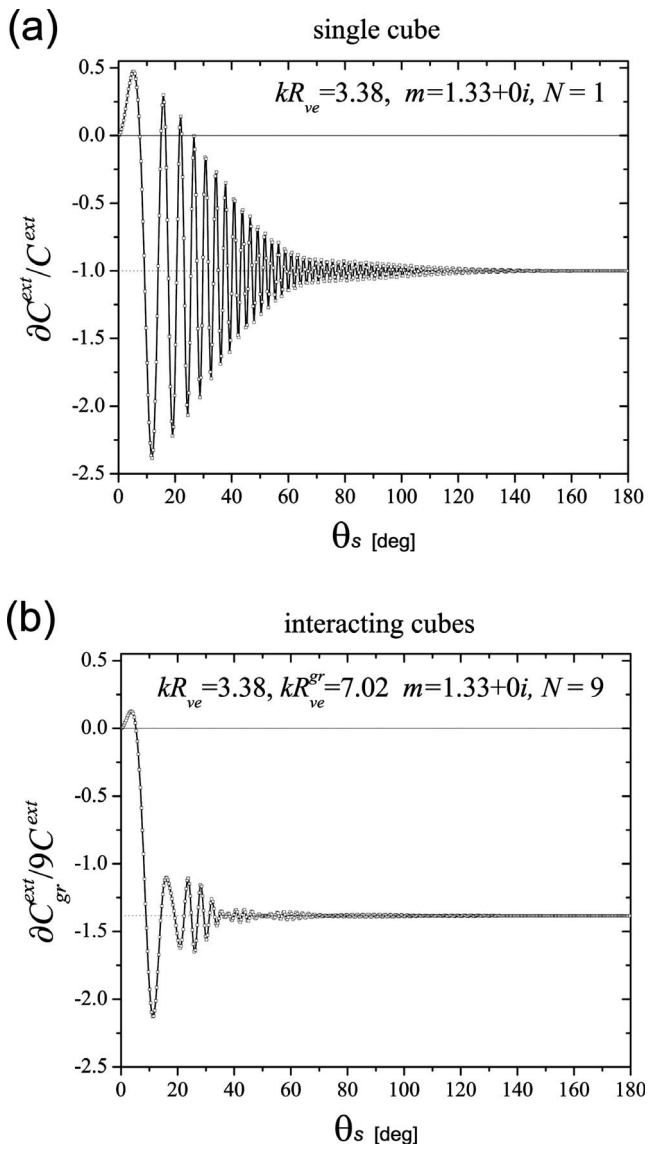

Fig. 5. Plots of ∂C_{gr}^{ext} given in Eq. (29) for a single cube (a) and the interacting cubical particle group (b). In plot (a) the curve is normalized by the single-particle extinction cross section C^{ext}, whereas the curve in plot (b) is normalized by $9C^{ext}$.

Figure 5(b) shows the integrated energy flow ∂C_{gr}^{ext} for the entire interacting particle group. Here the curve is normalized by nine times the single-particle extinction cross section. The qualitative effect of the presence of multiple particles is exactly the same as before; the dominant contribution to the group's extinction is compressed into a narrower angular region around the forward direction as compared to that of a single constituent particle. Inspection of Fig. 5(b) reveals that the curve converges to a value slightly greater than −1. This shows that the particle group extinction cross section C_{gr}^{ext} is greater than what would be expected in SSA from Eq. (26). Note that this increase is not necessarily a general feature of the effect of interparticle interactions on the extinction cross section; see [3] for more detail.

To further investigate the effect of interparticle interactions, Fig. 6 shows ∂C_{gr}^{ext} normalized by $9C^{ext}$ for the

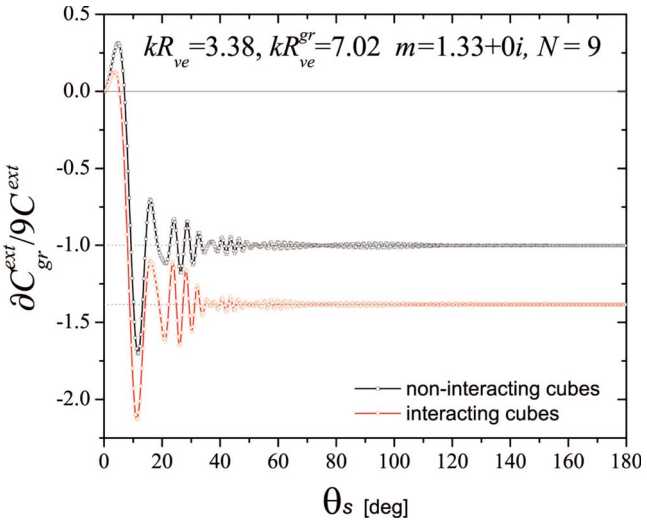

Fig. 6. (Color online) Plot of the integral ∂C_{gr}^{ext} given in Eq. (29) for the cubical particle group when the particles are treated as noninteracting and interacting. Both curves are normalized by $9C^{ext}$, where C^{ext} is the extinction cross section of a single cubical particle.

group when the particles are treated as both noninteracting and interacting. Comparison of the two curves shows that the larger value of C_{gr}^{ext} for the interacting group comes from slight increases and decreases in the magnitude of the integrated energy flow. This indicates that here the primary influence of the interparticle interactions occur mostly in the immediate neighborhood of the forward direction.

5. CONCLUSION

This work studies the extinction due to noninteracting and interacting multiparticle groups. As compared to a single particle, the effect of multiple particles is to narrow the angular region around the forward direction over which the dominant contribution to the group's extinction cross section occurs. This resolves an apparent inconsistency in Part I regarding the use of Beer's law to measure the extinction coefficient of dilute colloidal and aerosol systems. The effects of interparticle interactions on a particle group's extinction are studied using the DDA. The interactions are found not to change the essential character of the interference-based energy flow mechanism that describes the extinction.

ACKNOWLEDGMENTS

The authors are thankful for the useful comments of the two reviewers. This work was supported by the NASA Graduate Student Researchers Program.

REFERENCES

1. M. J. Berg, C. M. Sorensen, and A. Chakrabarti, "Extinction and the optical theorem. Part I. Single particles," J. Opt. Soc. Am. A **25**, 1504–1513 (2008).
2. M. I. Mishchenko, L. Liu, and G. Videen, "Conditions of applicability of the single-scattering approximation," Opt. Express **15**, 7522–7527 (2007).
3. M. I. Mishchenko, L. D. Travis, and A. A. Lacis, *Multiple Scattering of Light by Particles: Radiative Transfer and Coherent Backscattering* (Cambridge U. Press, 2006), Secs. 7.1 and 7.2.
4. P. A. Martin, *Multiple Scattering: Interaction of Time-Harmonic Waves with N Obstacles* (Cambridge U. Press, 2006), p. 2.
5. M. I. Mishchenko, J. W. Hovenier, and D. W. Mackowski, "Single scattering by a small volume element," J. Opt. Soc. Am. A **21**, 71–87 (2004).
6. M. I. Mishchenko, "Far-field approximation in electromagnetic scattering," J. Quant. Spectrosc. Radiat. Transf. **100**, 268–276 (2006).
7. C. T. Tai, *Dyadic Green Functions in Electromagnetic Theory* (IEEE, 1994), Sec. 4.
8. H. C. van de Hulst, *Light Scattering by Small Particles* (Dover, 1981), Sec. 4.22.
9. C. M. Sorensen, "Light scattering by fractal aggregates: a review," Aerosol Sci. Technol. **35**, 648–687 (2001).
10. A. Guinier and G. Fournet, *Small-Angle Scattering of X-Rays* (Wiley, 1955), p. 28.
11. M. A. Yurkin and A. G. Hoekstra, "The discrete dipole approximation: an overview and recent developments," J. Quant. Spectrosc. Radiat. Transf. **106**, 558–589 (2007).